Conformation Studies of Biologically Active Fragments of Bovine Growth Hormone†

Chen-jung Hsu Chen‡ and Martin Sonenberg*

ABSTRACT: Conformations of bovine growth hormone active fragments were studied using far ultraviolet circular dichroism and intrinsic fluorescence emission spectroscopy. The small fragment, A-II (segment 96–133 of bovine growth hormone), undergoes a helix to random coil structural transition between pH 5 and 10 (pK_a = 7.15). At pH 9, the random coil state of A-II reverts back to helix conformation as ionic strength increases from 0.01 to 1. The A-II fluorophore, Tyr-110, is quenched by a neighboring carboxyl group of Glu-111, but is only slightly affected by the secondary structural transition. The large fragment, A-I (segments 1–95 and 134–191, connected via a disulfide linkage, of bovine growth hormone), is a rigidly structured molecule with a large amount of β-sheet structure. Trp-86 of A-I was found to reside in an aromatic and hydrophobic amino acid cluster which is only destroyed by a high concentration of denaturant. Based on the primary sequence of bovine growth hormone, conformation predictions were made using the Chou–Fasman method ((1974) *Biochemistry 13,* 222). Bovine growth hormone helical structures are predicted to be in segments 10–34, 66–87, 111–127, and 186–191. β-Sheet structures are predicted to be in segments 45–54, 90–94, 101–105, 136–142, 161–165, and 174–179. Tetrapeptides 37–40, 41–44, 60–63, 129–132, 146–149, and 156–159 were predicted to be β turns. The prediction scheme confirmed several spectroscopic observations, but it did not completely explain the behavior of bovine growth hormone peptide fragments.

From partial tryptic digests of bovine growth hormone (bGH),[1] a homogeneous component (TbGH-d) was isolated and found to possess growth hormone activity (Sonenberg et al., 1968). TbGH-d is the result of peptide bond cleavages at positions 95–96 (Arg-Val) and 133–134 (Arg-Ala) within the bGH large disulfide loop. TbGH-d was further dissociated in 50% (v/v) acetic acid followed by gel filtration to yield two fragments: A-I (mol wt 15 000) and A-II (mol wt 5000) (Yamasaki et al., 1970).

The small peptide, A-II (bGH-(96–133)), demonstrated significant amounts of growth promoting activity (tibia width and weight gain assays) (Yamasaki et al., 1970) and stimulated hGH-like metabolic effects in humans (Levine et al., 1973b). The large peptide, A-I (bGH-(1–95, 134–191)), possessed little biological activity (Yamasaki et al., 1970).

Circular dichroism (CD) showed that, at pH 9.5, A-II is a random coil peptide and A-I contains mainly β-sheet conformation (Sonenberg and Beychok, 1971) in contrast to the parent molecule bGH which contains 45–50% helix (Sonenberg and Beychok, 1971; Bewley and Li, 1972; Holladay et al., 1974). These results raised interesting questions regarding the relationship between the hormone conformation and its biological activity. In order to further study this relationship, CD and fluorescence spectroscopy were used to investigate the conformational behavior of the active fragments, A-I and A-II. The results of our investigation are described in this paper. The prediction of bGH, A-I, and A-II conformations based on the primary sequence of bGH using the Chou–Fasman method (Chou and Fasman, 1974a,b) is presented.

Experimental Procedures

Materials

Bovine growth hormone was prepared by the method of Dellacha and Sonenberg (1964). The d component of the tryptic digest of bovine growth hormone (TbGH-d) was prepared by the method reported by Yamasaki et al. (1970). Sephadex was obtained from Pharmacia Fine Chemical, Inc., Piscataway, N.J. Urea for spectroscopic studies was the ultra pure grade of Schwarz/Mann Co., Orangeburg, N.J. Guanidine hydrochloride was the ExP grade by Heico, Inc., Delaware Water Gap, Pa. The Folin–Ciocalteau reagent for micro-Lowry protein determination was obtained from Fischer Scientific Co., Fair Lawn, N.J. All other reagents used were reagent grade. Glass-distilled water was used.

Methods

Isolation of the Biologically Active Fragments. Growth hormone active fragments, A-I and A-II, were isolated using the method described by Yamasaki et al. (1970). TbGH-d was chromatographed on a Sephadex G-75 column (2.5 × 90 cm) equilibrated with 35% (v/v) acetic acid aqueous solution at 4 °C. A-I and A-II fractions were further purified by rechromatography on the same column. The purities of the peptide fragments were established by disc electrophoresis and amino acid analysis.

Circular Dichroism Measurements. The far-UV CD spectra were obtained with a Cary Model 60 recording spectropolar-

† From the Memorial Sloan-Kettering Cancer Center, New York, New York 10021. *Received May 3, 1976.* Supported in part by Grants CA-08748 of the National Institutes of Health and BC-147 of the American Cancer Society.

‡ Part of a dissertation submitted by C.H.C. in partial fulfillment for the requirement of the degree of Doctor of Philosophy, Graduate School of Medical Sciences, Cornell University. Present address: Department of Pathology, Yale University School of Medicine, New Haven, Connecticut 06510.

[1] Abbreviations used: bGH, bovine growth hormone; hGH, human growth hormone; TbGH-d, d component of the partial tryptic digest of bovine growth hormone; A-I, 16 000 molecular weight fragment of bovine growth hormone (segments 1–95 and 134–191 connected via a disulfide bridge); A-II, 5000 molecular weight fragment of bovine growth hormone (segment 96–133); Gdn·HCl, guanidine hydrochloride; CD, circular dichroism; HoAC, acetic acid; v/v, volume by volume; UV, ultraviolet; IR, infrared. The abbreviations for amino acids conform to the tentative rules of the IUPAC-IUB Commission on Biochemical Nomenclature, as published ((1972) *J. Biol. Chem. 247,* 323).

imeter equipped with a circular dichroism attachment 6002, at 37 °C. The measured ellipticity, θ, in degrees, was normalized to molar residue ellipticity (deg cm^2/dmol) using a mean residue weight of 115. Cylindrical quartz cuvettes of path length 0.1 and 0.2 cm were generally used for spectrum measurements, recording at time constant 1 and range of 0.1 or 0.04. The sample protein solutions (0.1–0.2 mg/mL) were usually dissolved in 0.01 M ammonium bicarbonate buffer (pH 9) or 0.01 M ammonium formate buffer (pH 4). Protein concentrations were determined by the micro-Lowry method (Lowry et al., 1951) using bovine serum albumin as protein standard. CD spectra were analyzed using the method of Chen et al. (1972) based on eq 1 and constraints (eq 2a and 2b).

$$Y_i = f_\alpha X_{\alpha i} + f_\beta X_{\beta i} + f_c X_{ci} \quad i = 1, 2 \ldots N \tag{1}$$

$$f_\alpha + f_\beta + f_c = 1 \tag{2a}$$

$$0 \leq f_j \leq 1 \qquad j = \alpha, \beta, c \tag{2b}$$

where $X_{\alpha i}$, $X_{\beta i}$, and X_{ci} are the standard reference ellipticity values of the helix, β-sheet, and random structures (obtained from Table V, Chen et al., 1972), respectively, at a given wavelength. f_α, f_β, and f_c are fractions of helix, β-sheet, and random coil structures in the protein under investigation. Y_i is the protein experimental CD spectrum ellipticity value at a given wavelength. A nonlinear[2] least-squares analysis by means of stepwise Gauss–Newton iteration was used in order to best fit the spectral data Y_i and also adhere to constraint (eq 2b). The protein spectrum was analyzed in the wavelength region 243 to 201 nm at 3-nm intervals. The computations involved the use of an IBM 360/67 computer and the BMDX 85 statistical package (Dixon, 1968).

Fluorescence Spectroscopy. Fluoresence measurements were made on a Cary 50-026-900 differential spectrophotofluorimeter equipped with a thermostated cell compartment at 37 °C. Front surface illumination optics were used with a 23° angle between the exciting and emitting beam. The fluorescence intensity was corrected for fluctuations in illumination intensity. Variation in monochromator transmission and photomultiplier response with wavelength were also corrected for instrumentation. For emission spectra, samples in 0.5-cm quartz cuvettes were excited at 275 nm (bandwidth, 3.5 nm) and recorded from 420 to 280 nm (bandwidth, 8.6 nm). Spectral tracings were run in duplicate. Fluorescence intensity is presented on an arbitrary scale, i.e., relative fluorescence intensity mg^{-1} mL^{-1}.

Spectrophotometric Titration. The pH titrations (Liberti et al., 1969) were performed using a Radiometer Model TTT 1b pH meter. The protein solution (0.2 mg/mL of A-II in 0.1 N KCl, pH 2.7) was titrated with carbonate-free 0.1 N NaOH in 0.1 N KCl solution in a CO_2-free environment. Aliquots were taken for CD and fluorescence measurements and protein determination at every pH interval. The pH of the titration solution was read before and after the spectral measurements and the average values were used for plotting titration curves. A-I was titrated by the same procedure, except that it precipitated around pH 5–8. A small volume of 2 N KOH was added to dissolve the suspension and the titration was then carried out in the reverse direction from pH 12 to 9, using 0.1 N HCl.

The theoretical fluorescence titration curve was calculated based on the Henderson–Hässelbach equation (Edelhoch et al., 1966, 1967). The pK_a of each region of the titration curve is determined by finding the midpoint of the sigmoidal curve where half of the intensity changes had taken place assuming a single group ionization was responsible for each region of fluorescence quenching. Total fluorescence quenching in each region (in relative fluorescence intensity per mM) was used as the equivalent of total ionization. Three segments of the curve were generated using pK_a = 4.55, 7.05, 10.05 and total intensities 10.0, 1.93, and 9.33, respectively (Figure 4). The entire calculated fluorescence titration curve was produced by piecing together the three regions. The computation was done from pH 2 to 12 at 0.5 pH unit intervals with the aid of an IBM 360/67 computer.

Attempts were made to fit the CD titration curve (Mihalyi, 1970), using the above described method and three curves were generated (Figure 5): (a) assuming one group ionizing at pK_a = 7.15; (b) assuming two kinds of groups with equal populations ionizing at pH 6.35 and 7.95 (the average value of pK_a is still 7.15ΔpK_a = 1.6); (c) assuming two groups ionizing at pH 5.95 and 8.35 (ΔpK_a = 2.4). All three curves were computed from pH 3 to 12 at 0.3 pH intervals.

Effect of Denaturants on A-I and A-II Conformations. CD and fluorescence spectra of the active fragments in 4 M urea, 6.5 M urea, and 5 M guanidine hydrochloride (Gdn·HCl) in acidic and alkaline conditions were recorded. The ionic strength dependence of A-II conformations was also investigated at pH 4 and pH 9 in ionic strengths 0.01, 0.05, 0.1, 0.5, 1.0, and 2.0 NaCl solutions.

Predicting Molecular Conformation Based on Primary Structure. All amino acids in the bGH sequence (Gráf and Li, 1974b) were assigned as formers (H,h), breakers (B,b), and indifferents (I,i) for both helical and β-sheet structures according to Table I of Chou and Fasman (1974b). As shown in Figure 10, the region of helix nucleation was found at residues 20–25 by rule A-I (Chou and Fasman, 1974b). The helix was extended along both directions of the sequence until terminated by tetrapeptides 6–9 $(Hi_2B)_\alpha$ and 34–37 $(i_2bI)_\alpha$ according to rule A-2. Arg^+ is preferred at the C-terminal end (rule A-4) so Arg^+ -34 was incorporated into the helix and 10–34 was predicted to be helix structure. The same method (rule B) was applied to β-sheet structure. Whenever there were overlaps of helix and β-sheet regions, the average value of P_α and P_β of the segment (plus two residues on each side) $\langle P \rangle_\alpha$ and $\langle P \rangle_\beta$ were computed and the hierarchial structure was selected according to rules 1 and 2. The β turn tetrapeptides were selected by computing $\langle P_t \rangle$ using Tables VIII and P_t using Table VII of Chou and Fasman (1974b).

$$P_t = f_i f_{i+1} f_{i+2} f_{i+3} \tag{3}$$

where f_i, f_{i+1}, f_{i+2}, and f_{i+3} are respectively the frequency of occurrence for a certain residue at the 1st, 2nd, 3rd, and 4th position of a β turn. A tetrapeptide was chosen as β turn, if it satisfied the following conditions $\langle P_\alpha \rangle < 0.9$, $\langle P_t \rangle > \langle P_\beta \rangle$, and $P_t > 0.5 \times 10^{-4}$. Segments 37–40 and 146–149 were assigned as β turns due to the unusually high P_t values. Segment 129–132 was assigned as β turn since the difference between

[2] Using Gauss–Newton iteration (Draper and Smith, 1966), BMDX 85 linearized the regression equation by a Taylor's series expansion (zero and first-order terms) around the initial estimates of the parameters (f_α, f_β). In this particular case, the expansion is exactly our regression equation; therefore, the iteration converged at the second iteration. The result is the same as a linear regression analysis result (Chen, 1976). The difference is that BMDX 85 imposes constraints (eq 2b) on the computation, so that the results will retain physical meaning. In linear regression analysis, no constraints were placed on f_α and f_β, so that a few spectra produced negative f_β values, whereas BMDX 85 gives zero values for these cases. All cases with positive coefficients result in very close correspondence between linear regression and BMDX 85. Therefore, linear regression analysis programs, which are readily available, can be used when parameters obtained are within the domain dictated by constraints (eq 2b).

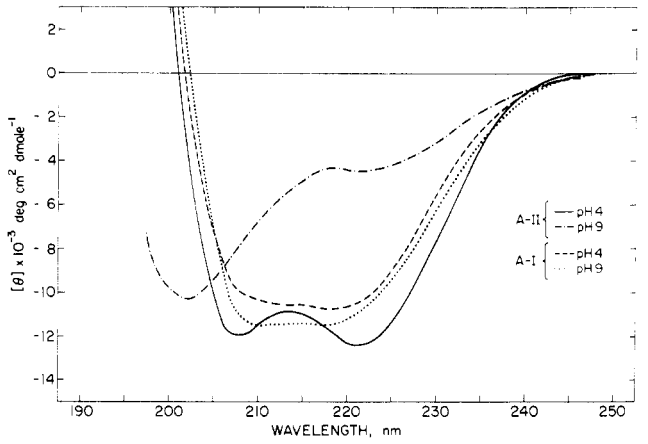

FIGURE 1: CD spectra of A-II and A-I. (—) A-II (0.209 mg/mL) in 10^{-2} M formate buffer (pH 4.0). (-----) A-II (0.22 mg/mL) in 10^{-2} M bicarbonate buffer (pH 9.0). (- - -) A-I (0.174 mg/mL) in 10^{-2} M formate buffer (pH 4.0). (···) A-I (0.161 mg/mL) in 10^{-2} M bicarbonate buffer (pH 9.0). The signal-to-noise ratios at 222 nm were 35:1 and 15:1 at 207 nm for A-II spectra. The signal-to-noise ratios at 215 nm were 20:1 for A-I spectra. Path length = 1 mm.

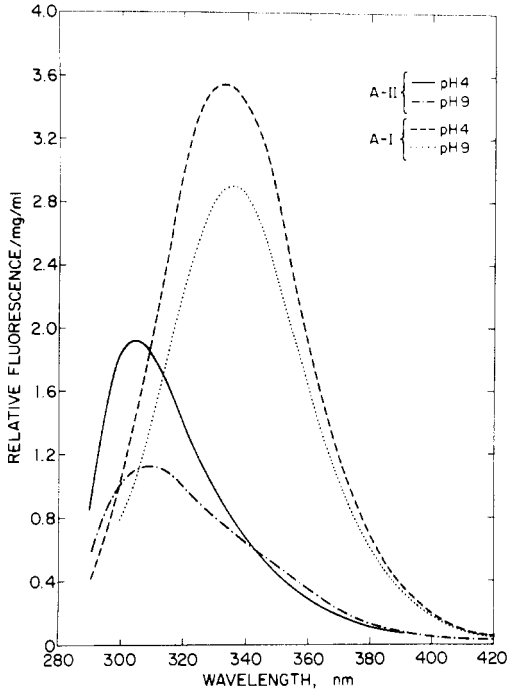

FIGURE 2: Fluorescence emission spectra of A-II and A-I. (—) A-II (0.076 mg/mL) in 10^{-2} M formate buffer (pH 4.0). (-----) A-II (0.188 mg/mL) in 10^{-2} M bicarbonate buffer (pH 9.0). (- - -) A-I (0.084 mg/mL) in 10^{-2} M formate buffer (pH 4.0). (···) A-I (0.223 mg/mL) in 10^{-2} M bicarbonate buffer (pH 9.0). Excitation wavelength was 275 nm. Excitation bandwidth was 3.3 nm. Emission bandwidth was 8.6 nm. The signal-to-noise ratio at 305 nm was 20:1 for A-II spectra and at 335 nm was 20:1 for A-I spectra.

$\langle P_t \rangle$ and $\langle P_\beta \rangle$ is the largest. The schematic diagrams of the helix, β-sheet, and β-turn regions predicted in bGH were made according to the ratio of the lengths of the helix, β-sheet, and random coil (Dickerson and Geis, 1969).

Results

CD and Fluorescence Spectra of the Active Peptides. The A-II CD spectrum at pH 4.0 (Figure 1) shows two troughs at 222 and 207.5 nm with a crossover at 201 nm which are typical of a helical spectrum. At pH 9.0, the A-II spectrum with two

TABLE I: Secondary Structure Parameters Analysis of the bGH Active Fragments.

Protein	pH	Helix[a]	β[a]	Random coil[a]
A-II	4	32	10	58
A-II	9	7	6	87
A-I	4	26	29	45
A-I	9	29	29	42
bGH	9.5	63	2	34

[a] Calculated from CD spectra of the active peptides using the least-squares fit method reported by Chen et al. (1972). Values expressed in percent.

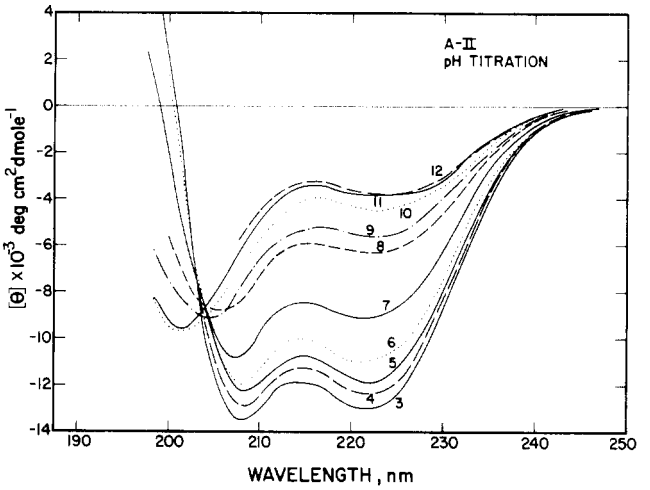

FIGURE 3: CD spectra of A-II titration at pH 3 to 12. A-II (0.2 mg/mL) was in 0.1 N KCl and titrated with 0.1 N KOH. The signal-to-noise ratios at 222 nm were 35:1 to 10:1 with increasing pH. The signal-to-noise ratios at 208 nm were 20:1 to 13:1 from pH 4 to 11. Path length = 2 mm.

low ellipticity negative extrema at 223 and 202 nm resembles a random coil protein. The A-I CD spectra in acidic and alkaline conditions (Figure 1) are very similar, with a broad trough between 220 and 210 nm and a crossover at 204 nm, indicating the presence of a β-sheet structure. CD spectral analyses using the method of Chen et al. (1972) are shown in Table I. A-II (containing no tryptophan) (Yamasaki et al., 1970) exhibits a typical tyrosine fluorescence emission spectrum with λ_{max} = 305 nm (Figure 2). A-I (containing 1 tryptophan and 5 tyrosines (Yamasaki et al., 1970)) shows a tryptophan fluorescence spectrum with emission maximum blue-shifted to 335 nm and no tyrosine emission characteristics.

Spectrophotometric Titration. A-II CD spectra show that a helix-to-coil transition took place in the A-II conformation, when the pH changed from 5 to 9 (Figure 3). The plot of $[\theta]_{222}$ as a function of pH (Figure 4) shows that there is little structural change at pH 3 to 5 and pH 10 to 12 and the transition curve is sigmoidal in shape with a point of inflection at pH 7.15. Calculated CD titration curves a, b, and c (Figure 5) did not fit the experimental data points, indicating that the helix-to-coil transition can not be accounted for by the simplified assumptions made in the computation.

The A-II fluorescence titration curve (Figure 4) displays three stages of intensity change with pK_a at 4.55, 7.05, and 10.05. In the acidic region, where there is no appreciable CD change, the tyrosine fluorescence intensity decreased by one-half. At alkaline pH, the tyrosine ionization had no influence

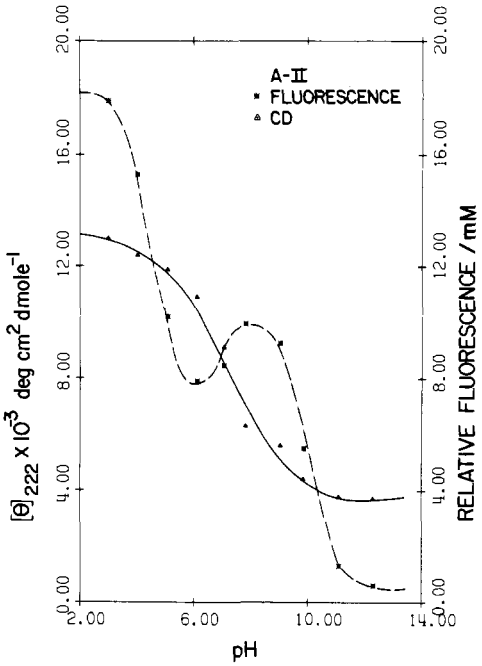

FIGURE 4: CD and fluorescence titration curves of A-II peptide. The CD titration curve (see Figure 3) is presented as $[\theta]_{222}$ (△ - - - △). The fluorescence emission at 305 nm was expressed as relative fluorescence intensity per mM of A-II peptide. (*) The experimental data points. (—) The theoretical fluorescence titration curve as explained in Methods. Fluorescence emission spectra were recorded with excitation at 275 nm, emission bandwidth 8.6 nm, and excitation bandwidth 3.3 nm. The signal-to-noise ratios at 305 nm were 30:1 at pH 4 and 15:1 at pH 9.

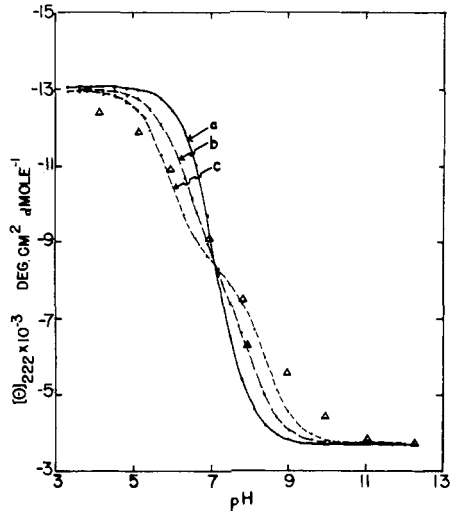

FIGURE 5: Theoretical curve fitting for CD titration curve. Curve a was generated with pK_a = 7.15. Curve b was generated using pK_a = 6.35 and 7.95. Curve c was the result of pK_a = 5.95 and 8.35. (△) The experimental data points.

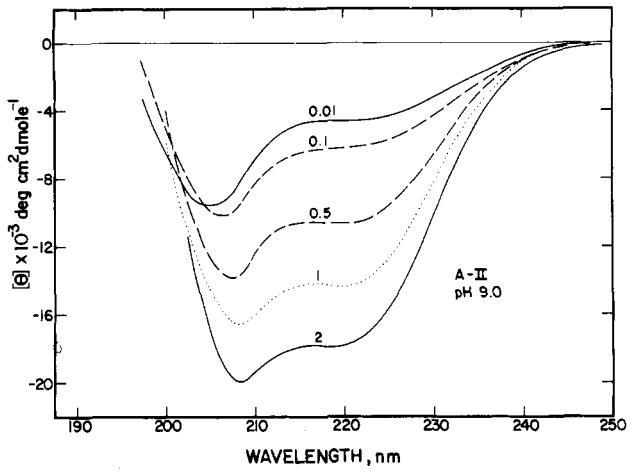

FIGURE 6: A-II CD spectra at varying ionic strength (pH 9). A-II solutions were about 0.210 mg/mL in 10^{-2} M bicarbonate buffer and contained NaCl in the following concentrations: 2 M (—), 1 M (···), 0.5 M (- - -), 0.1 M (- · -), and 0.01 M (—). The signal-to-noise ratios at 222 nm were 25:1 for the first two curves and 15:1 for the last three curves. The signal-to-noise ratios at 208 nm were 25:1 for the first two curves and 10:1 for the last three curves. Path length = 1 mm for all spectra.

on the CD spectra. There are corresponding changes between the two curves at neutral pH, but the magnitude of tyrosine fluorescence enhancement is small in comparison with the dramatic conformational change displayed by the CD spectra. The theoretical fluorescence titration curve (Figure 4) is generated by assuming only one group ionizing at pK_a = 4.55, 7.05, and 10.05 for the three regions, respectively. It agrees extremely well with the experimental data points, except for the neutral portion of the curve, where the experimental points are somewhat deviant. This deviation is also found in CD curve fitting, implying that more factors are involved in the neutral zone transition than just a single group ionization effect.

The A-I titration was interrupted by the precipitation of the peptide around its isoelectric point (between pH 5 and 8). The CD spectra at pH 3, 4, and 10 are very similar; all display a broad band between 210 and 220 nm $[\theta]$ of −10 000, −10 600, and −11 500, respectively, and a crossover at 202 nm. The pH 11 and 12 spectra resemble the pH 10 curve. The A-I fluorescence spectra show a quenching effect (half of the total intensity) in the alkaline range and it is associated with a gradual spectral shift of 4 to 340 nm with increasing pH. This change was not closely associated with any secondary structure change as shown by the CD curve.

Ionic Strength Dependence of A-II Conformation. The CD spectra of A-II at pH 4.0 with varying ionic strengths (μ) show the general characteristics of a helical spectrum. The $[\theta]_{222}$ increases from 15 000 to 19 000 and $[\theta]_{208}$ from 16 900 to 20 400 as ionic strength changes from 0.01 to 1. The corresponding fluorescence spectra exhibit a gradual increase in intensity at 305 nm as ionic strength changes from 0.01 to 0.5. A-II became insoluble in 1 M salt at pH 4.0. The random coil form of A-II (Figure 6) shows a progressive random coil to helix change with increasing ionic strength from 0.01 to 2 at pH 9. No precipitation was observed at high ionic strength in alkaline pH. The $[\theta]_{222}$ changed from 4500 to 17 800 and $[\theta]_{205}$ changed from 8700 to 20 000. The second trough at 205 nm was shifted to 206.5 nm and finally to 208 nm which is typical of the helical protein spectrum. The first trough at 222 nm was also shifted finally to 220 nm in 2 M salt. The helical content changes from 8 to 48% (Table II). In contrast to the dramatic CD spectral transition, the relative fluorescence intensity (Figure 7) of A-II under these conditions remains the same and there is a red shift from 305 nm (μ = 0.01) to 310 nm at higher ionic strengths.

Effect of Denaturants on A-I and A-II Conformations. Gdn·HCl, 5 M, and 6.5 M urea reduced the CD spectra of both A-II and A-I under all conditions to featureless lines resembling a random coil protein spectrum. Urea (4 M) only destroyed 10% of the ellipticity of A-II at pH 4, which was originally in the helix state, but the random coil state of A-II at pH 9 has been changed to a spectrum similar to that treated with Gdn·HCl. A-I structure at pH 9 is resistant to 4 M urea

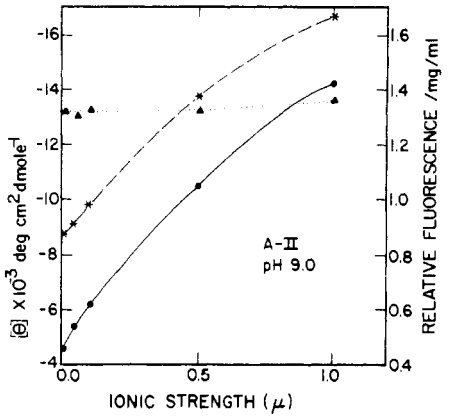

FIGURE 7: Ionic strength dependence curve of A-II conformation parameters at pH 9.0. $[\theta]_{222}$ (—); $[\theta]_{208}$ (- - -); and relative fluorescence mg^{-1} mL^{-1} at 305 nm (···).

TABLE II: CD Spectral Analysis of A-II in Varying Ionic Strengths.[a]

Ionic strength	pH	Helix	β	Random coil
0.01	9	8	16	76
0.1	9	13	8	79
0.5	9	27	9	64
1.0	9	39	1	60
2.0	9	48	0	52
1.0	4	50	10	40

[a] Analyzed using method of Chen et al. (1972). Values expressed in percent.

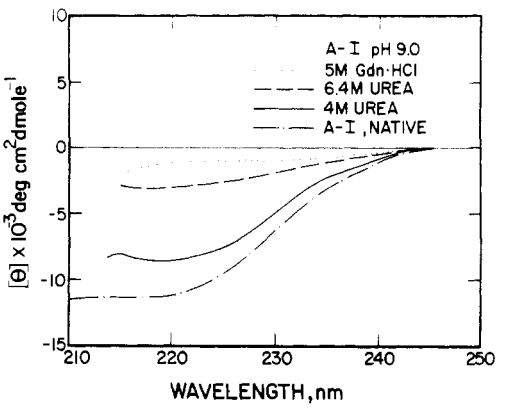

FIGURE 8: Effect of denaturants on A-I CD spectra at pH 9.0. The A-I solutions were 0.21 mg/mL in 10^{-2} M bicarbonate buffer (pH 9.0). The signal-to-noise ratios at 222 nm were 1.5:1 for the 5 M Gdn·HCl (···), 5:1 for the 6.5 M urea (- - -), and 7:1 for the 4 M urea (—). (·····) A-I CD spectra at pH 9.0. Path length = 1 mm for all spectra.

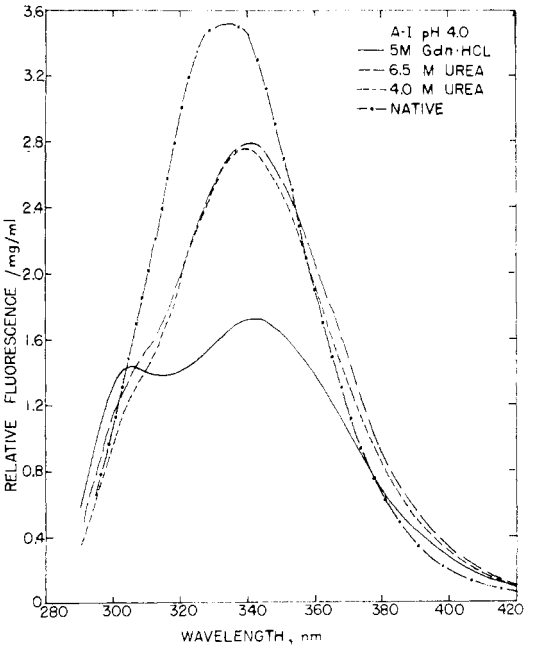

FIGURE 9: Effect of denaturants on A-I fluorescence at pH 4. A-I solutions were 0.21 mg/mL in 10^{-2} M formate buffer (pH 4). The signal-to-noise ratios at 335 nm were 30:1 for the Gdn·HCl curve (—) and 6.5 M urea curve (— —), 20:1 for the 4 M urea curve (- - -), and at 305 nm was 35:1 for the Gdn·HCl curve. (·····) Native A-I at pH 4. Excitation at 275 nm. Excitation band width was 3.2 nm. Emission bandwidth was 8.6 nm.

with only 20% of the ellipticity abolished (Figure 8), but at pH 4 the A-I spectrum has been changed to a random coil spectrum. The fluorescence spectra of A-I in pH 4 (Figure 9) show that treatment with 5 M Gdn·HCl separated the 305-nm tyrosine peak from the tryptophan peak which was red shifted to 340 nm. Urea did not affect the spectral line shape, except for a slight shoulder at approximately 305 nm and a decrease in intensity from 3.6 to 2.8. Under alkaline conditions, 5 M Gdn·HCl also dissociated the original peak into a smaller tyrosine peak at 303 nm (intensity = 1.36) and the tryptophan peak at 342 nm (intensity = 1.92).

Conformation Prediction Based on Primary Amino Acid Sequence. The predicted secondary structure of bGH is shown in Figure 10. The $\langle P_\alpha \rangle$, $\langle P_\beta \rangle$, and $\langle P_t \rangle$ values used in the assignment of the helix, β-sheet and β-turn structures are shown in Table III. There are four segments of helix, 10–34, 66–87, 111–127, and 186–191; six β-sheet regions, 45–54, 90–94, 101–105, 136–142, 161–165, and 174–179. The schematic diagram (Figure 11) shows the predicted helix, β-sheet, and β-turn regions in the bGH molecule. The result is speculative since the bGH three-dimensional structure is as yet unknown. However, there are some interesting findings. The A-II helical region is predicted to be in segment 111–127 which does not include Tyr-110. Tyr-36, Tyr-43, Tyr-110, Tyr-143, and Trp-86 were positioned close together to enhance hydrophobic interaction in the tertiary structure. The two cysteine residues of the large disulfide loop are very far apart, but they both reside in β-sheet structure. The molecule would have to be folded a little to establish the disulfide bond and β-sheet interchain hydrogen bonds. The positions of tryptic cleavages at 95–96 and 133–134 (to form A-I and A-II) are found to be near the regions of β-pleated sheet and β-turn structures. By these predictions, bGH contains 37% helix and 20% β-sheet structure (based on the number of residues involved in the specific secondary structures); this could be compared with 62% helix and 3% β-sheet by Chen's method (bGH CD spectrum pH 9) and the generally recognized 50–55% helix (Sonenberg and Beychok, 1971; Bewley and Li, 1972; Holladay et al., 1974). Considering an 80% accuracy, the prediction of 37% helix in bGH is lower and the β-sheet result is slightly higher. A-II is predicted to contain 45% helix and 13% β structure. This is close to the A-II helical conformation at pH 4. A-I is predicted to contain 34% helix and 22% β sheet which is different from the predominantly β-sheet structure shown by CD and infrared spectroscopy (Sonenberg and Beychok, 1971).

TABLE III: Predictive Data of Helix, β Sheet, and β Turn Regions in bGH.[a]

Peptide	$\langle P_\alpha \rangle$	$\langle P_\beta \rangle$	$\langle P_t \rangle$	$P_t \times 10^{-5}$	Assignment	Comment
10-34	1.21	0.99			α helix	34-37, 6-9 breaks
37-40	0.91	0.82	1.06	11.1	β turn	
41-44	0.84	1.04	1.09	7.4	β turn	
45-54	1.05	1.24			β sheet	40-44 breaks
60-63	0.85	0.9	1.16	8.4	β turn	
66-87	1.17	1.03			α helix	
90-94	0.98	1.07			β sheet	
97-100	0.86	0.96	1.24	5.9	β turn	
101-105	0.99	1.5			β sheet	97-100, 106-109 break
111-127	1.24	0.9			α helix	107-110, 129-132 breaks
129-132	0.73	0.86	1.37	4.3	β turn	
136-142	1.03	1.22			β sheet	132-135, 143-146 breaks
146-149	0.93	1.08	1.15	19.3	β turn	
156-159	0.93	0.98	1.12	6.7	β turn	
161-165	1.07	1.15			β sheet	157-160, 166-169 breaks
174-179	0.98	1.32			β sheet	170-173, 180-183 breaks
186-191	1.19	0.92			α helix	

[a] Values calculated by the Chou-Fasman method (1974b).

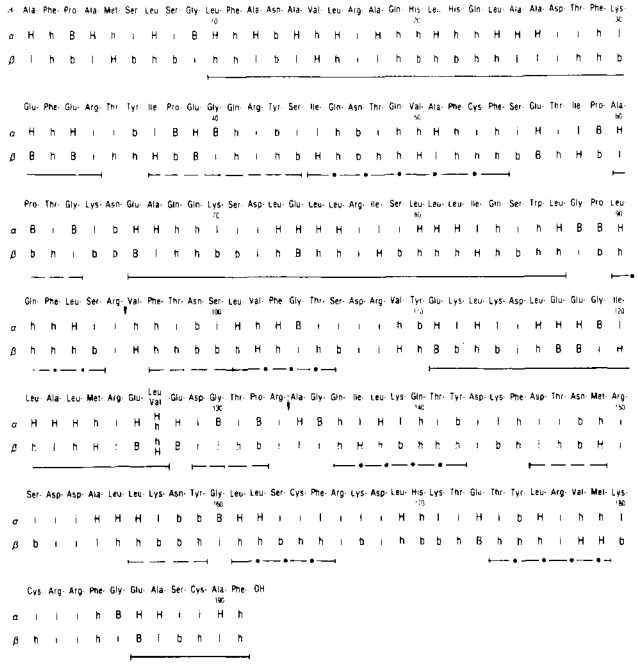

FIGURE 10: Predictive analysis of helix, β sheet, and β turn regions in bGH. Assignments in the first row under each residue refer to helical potential (P_α), and in the second row to β-sheet potential (P_β). H, strong former; h, former; i, indifferent; b, breaker; and B, strong breaker. (—) Predicted to be helix; (— ● —) β sheet; and (- - -) β turn. Unmarked areas are unspecific random coil regions.

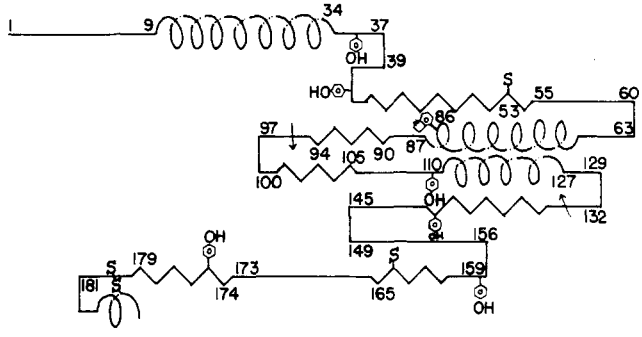

FIGURE 11: Schematic diagram of helical, β-sheet, and reverse β-turn regions predicted in bGH based on Figure 10. Segments are represented in their respective conformational states: helix (σ,''), β-sheet (vv), and random coil (—). Chain reversals denote β turn tetrapeptides. Conformational boundary residues are numbered. Four Cys residues indicated by S, and Tyr and Trp are represented by their side chain chemical formulas. The diagram was made according to the ratio of the length of the helix (5.41 Å/3.6 residues), antiparallel β-pleated sheet (6.95 Å/2 residues), and random coil (3.6 Å/residue). The length ratio per amino acid residue for the three conformations is helix: β-sheet; random coil = 0.42:0.96:1 (1.5:3.47:3.6 in Å). Each helical loop (σ'') represents a single turn consisting of 3.6 residues.

Discussion

Secondary structural parameter analysis of the CD spectrum of A-II at pH 4 shows that it contains 32% α-helix and 10% β-sheet conformation. Twelve residues are probably involved in the helical structure of this 38 amino acid peptide. The A-II spectrum at pH 9 is a typical random coil spectrum with 7% α-helix and 6% β-sheet structures. The A-II spectrum at pH 9.5 recorded by Sonenberg and Beychok (1971) shows a similar line shape and ellipticity. The corresponding fluorescence spectra display a normal tyrosine emission peak at 305 nm with low intensity compared with the fluorescence of the amino acid, tyrosine.

The CD titration curves of A-II show a helix to coil transition about pH 5 to 9 with the point of inflection at pH 7.15. The computed theoretical curves (Figure 4) failed to fit the experimental data, indicating that more side chain groups are responsible for the transition (Mihalyi, 1970). Examining the charge distribution of the A-II sequence (Figure 10) (Yamasaki et al., 1972, 1975) reveals that, at pH 3, there are 7 evenly distributed positive charges along the peptide chain. At pH 9, in addition to the 7 positive charges, there are 9 negative charges concentrated in segment 111-129 at the C-terminal portion of the A-II peptide. Conformation predictions based on the primary sequence show that the A-II helix region is predicted to be in segment 111-127.

The fluorescence behavior of A-II is more complicated than the single phase transition manifested by the CD titration. There is pronounced fluorescence quenching observed in the pH 3-5 region where carboxyl groups normally ionize. The fluorescence quenching is only partially (20%) reversed in the pH 5-9 region, which corresponds to the helix to coil secondary

structural transition. The fact that an overall secondary structure change did not completely abolish the quenching effect indicates that a major quencher is located close to the tyrosyl group at the primary structural level. Segment 109–112 has the following sequence: -Val-Tyr-Glu-Lys-. A γ-carboxyl group of the glutamic acid is adjacent to the tyrosine fluorophore. Theoretical curve fitting has shown that it is a single group ionizing at pH 4.55, which is just 0.3 unit away from the normal pK_α (4.25) of the γ-carboxyl group of glutamic acid. Therefore the first stage of the fluorescence titration curve is a close reflection of the ionization behavior of glutamic acid. The slight enhancement of fluorescence intensity at about pH 7.05 parallels the helix–coil transition demonstrated in the CD titration curve. This second stage of the fluorescence titration curve reflects the effect of a minor quencher, positioned within the quenching range of the tyrosine by the secondary conformation. When A-II changes into an extended coil structure, the quencher is removed and the fluorescence intensity is restored. The last part of the fluorescence titration curve demonstrates the behavior of a phenyl group ionization. Tyrosine quenching and ionization are not greatly affected by the helix–coil transition and tyrosine ionization does not cause any CD spectral change (Pesce et al., 1964). This implies that tyrosine is probably not in the helical region of the A-II molecule. Segment 111–127 is predicted to be helix based on the A-II sequence. Tyr-110 does not reside in this helical region.

Increasing ionic strength does not affect the A-II helical conformation, indicating that the A-II helical conformation is stabilized by increasing ionic strength. The A-II random coil conformation is greatly affected by ionic strength. The CD spectra display a progressive change from random coil to helix with increasing ionic strength. Neutral salt weakens the repulsive interaction between the ionized side chain and permits the formation of molecular inter- or intrachain hydrogen bonds to form a helical structure. The A-II random coil was completely denatured by concentrated urea and Gdn·HCl at alkaline pH. The A-II helical structure was not totally abolished by 4 M urea as it was with Gdn·HCl.

A-II has little structure in solution especially in the neutral and higher pH. It undergoes a helix–coil transition at neutral pH and its random coil conformation readily reverts back to helix at high ionic strength. A-II conformation in solution does not reflect its conformation in bGH. The A-II structure can be very different in the presence of A-I. This is observed in the S-peptide of ribonuclease (Richards et al., 1971), which is a structureless peptide in solution, but a major part of it is involved in the helix in the ribonuclease protein.

The CD spectra of A-I have almost identical line shapes at acid and alkaline pH. The trough between 220 and 210 nm suggests β-sheet characteristics. Analysis shows that the protein contains 26% α-helix, 29% β and 45% random coil. The existence of β structure is also supported by the infrared vibrational spectrum of bGH previously recorded (Sonenberg and Beychok, 1971). The A-I IR spectrum showed an amide I band at 1650 cm^{-1} and amide II band at 1535 cm^{-1} which correspond to the OH stretching of the intramolecular hydrogen bonding of the β-pleated sheet structure.

A-I fluorescence spectra display an emission maximum at 335 nm which indicates that tryptophan is imbedded in a hydrophobic environment surrounded by apolar amino acids. A-I contains five tyrosines and one tryptophan, but it displayed no tyrosine emission shoulder (303 nm) under either acid or basic conditions. Some of the tyrosine excitation energy must have undergone radiationless energy transfer to the tryptophan fluorophore. In order for a 50% energy transfer to occur, the critical distance (R_0) between the tyrosine and tryptophan should be around 13 Å (Edelhoch et al., 1967; Perlmann et al., 1968). This implies that probably most of the tyrosine side chains are located within the 13-Å vicinity of the tryptophan fluorophore. Therefore, a hydrophobic cluster of aromatic and other apolar amino acids could be formed in the A-I structure. The schematic diagram (Figure 4) also indicates that four tyrosine groups Tyr-36, Tyr-43, Tyr-110, and Tyr-143 (Tyr-110 is not included in A-I) are close to Trp-86 for such interaction. Eight residues on each side of Trp-86 (i.e., 78–85 and 87–94) are hydrophobic amino acids. They provide a highly hydrophobic environment for Trp-86 as indicated by the blue shift of the fluorescence spectrum of A-I at 335 nm as compared with the emission maximum at 350 nm for tryptophan in aqueous solution. The hydrophobicity of this area is also supported by the observation of Gráf and Li (1974b) in their sequence study. They found that fragments 78–98 and 1–17 formed aggregates characterized by strong hydrophobic interactions which were not separated by partition chromatography and high-voltage paper electrophoresis. The two peptides are probably associated at their helical regions.

A-I titration was interrupted due to protein precipitation around pH 5–8. bGH has an isoelectric point at pH 6.85 and it also becomes insoluble in the isoelectric region. A-I seems to possess some bGH properties. It is less soluble than bGH at neutral and slightly basic conditions. CD spectra show that the conformation of A-I in acidic and basic pH are very similar. The fluorescence intensities are different due to quenching by the ionized carboxyl group. bGH was also reported to exhibit no secondary structural change (far-UV CD spectra), while the aromatic chromophores displayed structure alterations (near-UV CD spectra) (Bewley and Li, 1972; Edelhoch and Lippoldt, 1970). The CD spectra of A-I at two different pHs are very similar, but the effect of denaturants on these two conformations are quite different. At pH 4, A-I is almost totally denatured by the chemicals, but A-I at pH 9 is able to resist the attack of 4 M urea and still retain some structure. The fluorescence spectra of A-I in Gdn·HCl show separation of the 305-nm shoulder from the tryptophan main peak (340 nm) which is appreciably smaller. Gdn·HCl has disrupted the protein conformation completely, thus decreasing the energy transfer between tyrosine and tryptophan and exposing the tryptophan to a more polar environment. Urea (4 M) does not affect the spectrum of A-I at pH 9, and 6.5 M urea does bring about a change in emission maximum to 340 nm. All these observations support the conclusion that A-I is a more structured molecule.

The present studies have not been able to identify the exact conformations of A-I and A-II in their native states in the parent molecule. The bGH structure predicted based on primary sequence shows that the A-II segment has helical structure, which is probably related to the A-II helical conformation state at pH 4 as observed by CD. A-I and A-II were shown to recombine in 1 N HoAC (Sonenberg et al., 1972; Hara et al., submitted). Since A-II is already in a helical conformation, it can be easily incorporated into the complex with some conformational adjustments. A-I contains a high percentage of β structure which was not present in bGH indicating that the A-I structure is different from the native A-I conformation originally in bGH. The lack of conformational flexibility of A-I indicates that it is frozen in the high β-structure state which is more difficult to revert back to native A-I in bGH. This may explain the observation that the A-I–A-II recombined complex (Hara et al., submitted; Chen, 1976) is higher in β-sheet content, lower in ellipticity, and lower in

biological activity than native TbGH-d and bGH.

The conformation predicted by the Chou–Fasman method has explained some of the phenomena found in chemical and spectroscopic studies. Figure 10 shows that bGH contains helix in segments 10–34, 66–87, 111–127, and 186–191. Holladay et al. (1974) used the semiempirical rules of Kotelchuck and Sheraga (1969) based on short range interactions to analyze ovine growth hormone (oGH). They predicted the α-helix regions in oGH involving residues 14–26, 29–34, 49–60, 73–97, 108–113, 116–130, 133–140, and 176–191, with a possible bend in 88–89. With the exception of segments 49–60, 133–140, and 176–186, the locations of the helix structures of the two predictions more or less overlap. Most of the expected helices are located within the N-terminal two-thirds of the protein. This is in agreement with their finding that the A–B cyanogen bromide fragments of growth hormone which comprise approximately two-thirds of the N-terminal portion of growth hormone have essentially the same degree of secondary structure as the intact molecule (Levine et al., 1973a).

The positions of tryptic cleavages at 95–96 and 133–134 are near the regions of β-pleated sheets and β-turn structures. These conformations are favorable for the formation of antiparallel pleated sheets type hydrogen bonds with the trypsin active sites (Stroud et al., 1971). These interactions bring the substrate Arg-Val or Arg-Ala amide bond into close proximity with the enzyme catalytic functional moieties imidazole of His-57 and hydroxyl of Ser-195, thus facilitating the serine protease mechanism of trypsin.

The A-II helix region is predicted to be in segment 111–127. The conformational integrity of the A-II was not destroyed by human plasmin cleavage at position 112–113 (Gráf and Li, 1974a). A-II cyanogen bromide fragments (Met-124 destroyed) remain associated as a complex which was dissociated by gel filtration in 50% acetic acid (Yamasaki et al., 1972).

Using the Chou–Fasman method to predict A-I and A-II structure gave different results from that obtained by Chen's CD calculation method. This discrepancy could be due to the following reasons: (a) their method did not take into account the solution property of protein; (b) their method did not consider the effect of pH on protein conformation; (c) it may not be reasonable to compare fragments (A-I and A-II) with the parent molecule (bGH). Table XIV of Chou and Fasman (1974b) shows a comparison between both methods. The predictive method gives higher helical and β-sheet contents in most cases. Helix or β-sheet structure assignment was sometimes ambiguous. Since P values for β sheet are higher than those calculated for helix, $\langle P_\beta \rangle$ was most likely higher than $\langle P_\alpha \rangle$; thus more β-sheet assignments were made in cases of an ambiguous situation. No P value was assigned for Asp, Glu, His, Cys-, and Tyr-. This method was used for protein at neutral pH. Therefore, the helix to random coil transition of A-II with pH changes cannot be predicted by this method. A-II was predicted to contain 45% helix, which describes the A-II helical (32% helix) state well in the acidic condition. The 45% helical content probably indicates the potential helix. In fact, A-II was shown to form 50% helix in high ionic strength as observed by CD spectroscopy.

Chou and Fasman have cautioned about applying their method to protein fragments, especially in aqueous solution states. A-I contains 80% of the bGH sequence and its CD spectrum is characteristic of β-sheet structure, whereas bGH has a predominantly helical structure. It is impossible to arrive at two very different conformations for A-I and bGH individually based on large amounts of common sequence. The disulfide region of the large loop could have been less strained due to the removal of A-II, and A-I may undergo rearrangement favoring more intrachain hydrogen bonding, i.e., β-sheets interactions possibly in segments 41–44, 60–63, 156–159, and 160–170, thus enhancing the β-sheet structure of the A-I peptide.

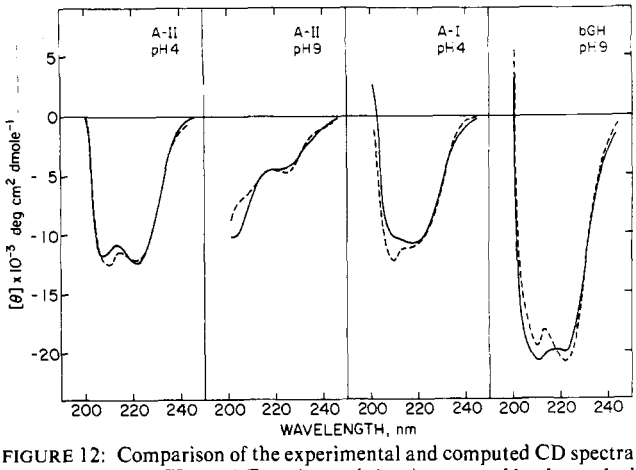

FIGURE 12: Comparison of the experimental and computed CD spectra of A-II, A-I, and bGH. (—) Experimental; (- - -) computed by the method of Chen et al. (1972).

As noted under Methods, the rules of predicting β-turn, in some instances, were not followed closely. Segments with unusually high values of $\langle P_t \rangle$ and $\langle P_\beta \rangle$ were scored as β turns. The prediction of an extra β turn will result in a completely different schematic diagram. Segment 89–97 has $\langle P_\beta \rangle < \langle P_\alpha \rangle$ but proline and arginine are not frequently found in β structures. This underscores the conflict between the methods of type assignment (H, B, I) to locate makers and breakers and the method of computing numerical averages of the probability of occurrence values and cutoff values.

Deviations from experimental CD spectra were found in curves computed by the method of Chen et al. (1972) (Figure 12) around 210 nm. The π–π^* band (Holzwarth and Doty, 1965) ellipticity values are perhaps improperly represented and refinements around this region might produce a better fit to the experimental spectrum. These deviations could also be caused by the dependence of α-helix CD band at 208 nm on chain length. Chen et al. (1972) computed the standard ellipticity values with proteins containing helix segments with an average of 9 residues per helix segment. In the case of bGH, the helical stretches are longer than the standard proteins, which may have resulted in a proportionally greater 208-nm band.

In conclusion, spectroscopic studies described in this paper show that the large fragment, A-I, is a nonpolar, rigidly structured molecule which did not undergo conformational change except with high concentrations of denaturant. The small peptide, A-II, is a very flexible and polar molecule which readily undergoes conformational rearrangement at varying pH and ionic strengths. The Chou–Fasman method seems to be valid for native globular proteins at neutral pH. The predictive model resembles the characteristics of protein in the solid state. Short chain, small peptide fragments do not fit the prediction. Chen's CD spectrum method is applicable for proteins in solution with varying pH and ionic strength and is suited for studying protein interaction in solution. But Chen's method was not valid for protein with no helix or β CD band.

Acknowledgments

The authors are grateful to Drs. Allan Schneider and Sol I. Rubinow for helpful criticisms.

References

Bewley, T. A., and Li, C. H. (1972), *Biochemistry 11,* 927.

Chen, C. H. (1976), Doctoral Dissertation, Cornell University.

Chen, Y. H., Yang, J. T., and Martinez, H. M. (1972), *Biochemistry 11,* 4120.

Chou, P. Y., and Fasman, G. D. (1974a), *Biochemistry 13,* 211.

Chou, P. Y., and Fasman, G. D. (1974b), *Biochemistry 13,* 222.

Dayhoff, M. O. (1972), Atlas of Protein Sequence and Structure, Vol. 5, Dayhoff, Ed., Silver Springs, Md., National Biomedical Research Foundation.

Dellacha, J. M., and Sonenberg, M. (1964), *J. Biol. Chem. 239,* 1515.

Dickerson, R. E., and Geis, I. (1969), The Structure and Action of Proteins, New York, N.Y., Harper & Row.

Dixon, W. J., Ed. (1968), University of California Automatic Computation B.M.D. X Series, p 177.

Draper, N. R., and Smith, H. (1966), Applied Regression Analysis, New York, N.Y., Wiley.

Edelhoch, H., Brand, L., and Wilcheck, M. (1967), *Biochemistry 6,* 547.

Edelhoch, H., Condliffe, P. G., Lippoldt, R. E., and Burger, H. G. (1966), *J. Biol. Chem. 241,* 5205.

Edelhoch, H., and Lippoldt, R. E. (1970), *J. Biol. Chem. 245,* 4199.

Gráf, L., and Li, C. H. (1974a), *Biochemistry 13,* 5409.

Gráf, L., and Li, C. H. (1974b), *Biochem. Biophys. Res. Commun. 56,* 168.

Hara, K., Chen, C. H., and Sonenberg, M., manuscript submitted.

Holladay, L. A., Hammonds, R. G., Jr., and Puett, D. (1974), *Biochemistry 13,* 1653.

Holzwarth, G., and Doty, P. (1965), *J. Am. Chem. Soc. 87,* 218.

Kotelchuck, D., and Scheraga, H. A. (1969), *Proc. Natl. Acad. Sci. U.S.A. 62,* 14.

Levine, J. H., Holladay, L. A., Nicholson, W. E., Puett, D., and Salman, W. D., Jr. (1973a), Abstracts of the 55th Annual Meeting of the Endocrine Society, Chicago, Ill.

Levine, L., Sonenberg, M., and New, M. E. (1973b), *J. Clin. Endocrinol. Metab. 37,* 607.

Liberti, J. P., Alfano, J., and Sonenberg, M. (1969), *Biochim. Biophys. Acta 181,* 176.

Lowry, O. H., Rosebrough, N. J., Farr, A. L., and Randall, R. J. (1951), *J. Biol. Chem. 193,* 265.

Mihalyi, E. (1970), *Biochemistry 9,* 804.

Perlman, R. L., van Zyl, A., and Edelhoch, H. (1968), *J. Am. Chem. Soc. 90,* 2168.

Pesce, A., Bodenheimer, J., Norland, K., and Fasman, G. D. (1964), *J. Am. Chem. Soc. 86,* 5669.

Richards, F. M., Wyckoff, H. W., Carlson, W. D., Allewelle, N. M., Lee, B., and Mitsui, Y. (1971), *Cold Spring Harbor Symp. Quant. Biol. 36,* 35.

Sonenberg, M., and Beychok, S. (1971), *Biochem. Biophys. Acta 229,* 88.

Sonenberg, M., Kitkutani, M., Free, C. A., Nadler, A. C., and Dellacha, J. M. (1968), *Ann. N.Y. Acad. Sci. 148,* 532.

Sonenberg, M., Yamasaki, N., Kikutani, M., Swislocki, N. I., Levine, L., and New, M. (1972), Growth and Growth Hormone, Pecile and Muller, Ed., Amsterdam, Excerpta Med. Found.

Stroud, R. M., Kay, L. M., and Dickerson, R. E. (1971), *Cold Spring Harbor Symp. Quant. Biol. 36,* 125.

Yamasaki, N., Kangawa, K., Kobayashi, S., Kikutani, M., and Sonenberg, M. (1972), *J. Biol. Chem. 247,* 3874.

Yamasaki, N., Kikutani, M., and Sonenberg, M. (1970), *Biochemistry 9,* 1107.

Yamasaki, N., Shimanaka, J., and Sonenberg, M. (1975), *J. Biol. Chem. 250,* 2510.